A Machine Learning Approach for Mapping Forest Categories: An Application of Google Earth Engine for the Case Study of Monte Sant'Angelo, Central Italy

Mattia Balestra[1], Stefano Chiappini[1(✉)], Eva Savina Malinverni[2], Andrea Galli[1], and Ernesto Marcheggiani[1,3]

[1] Dipartimento di Scienze Agrarie, Alimentari e Ambientali (D3A), Università Politecnica delle Marche, Via Brecce Bianche 10, 60131 Ancona, Italy
{m.balestra,s.chiappini}@pm.univpm.it, {a.galli, e.marcheggiani}@univpm.it

[2] Dipartimento d'Ingegneria Civile, Edile e Architettura (DICEA), Università Politecnica delle Marche, Via Brecce Bianche 12, 60131 Ancona, Italy
e.s.malinverni@univpm.it

[3] Department of Earth and Environmental Sciences, KU Leuven, 3001 Leuven, Belgium

Abstract. Remote Sensing plays a critical role in forest tree species identification. Regarding the current debate on earth observation and monitoring, many see this valuable technology useful for a wide range of purposes, including forest conservation and management. This paper focuses on a workflow for mapping forest tree species from satellite images, by statistic algorithms and machine learning. Among the world satellite platforms, the Sentinel-2 program was selected to investigate the mixed forest area of Monte Sant'Angelo in Central Italy. A list of monthly images from 2018 to 2020 have been processed using the Google Earth Engine geospatial processing service. The process includes the computation of vegetation indexes like the Normalized Difference Vegetation Index (NDVI), Transformed Difference Vegetation Index (TDVI), the Enhanced Vegetation Index (EVI) and the Green Normalized Difference Vegetation Index (GNDVI). A forest class time series was generated for each index. The Artificial Intelligence algorithm models (Machine Learning) were trained identifying accurate ground truths. Principal Component Analysis (PCA) was performed to reduce variables redundancy in Random Forest classifications. Four forest categories have been identified: holm oak woodlands, conifer reforestation, Ostryo Carpinion alliance and mixed hardwood forest. Due to the phenological differences among species, the classification global accuracy ranges from 70% to 80%.

Keywords: Google Earth Engine · PCA · Random forest · Sentinel-2 · Time-series · Tree species classification

© Springer Nature Switzerland AG 2021
O. Gervasi et al. (Eds.): ICCSA 2021, LNCS 12955, pp. 155–168, 2021.
https://doi.org/10.1007/978-3-030-87007-2_12

1 Introduction

Vegetation maps are a key tool to represent habitats patterns and their distribution. Monitoring is a critical to an effective conservation of the habitats (92/43/EEC Habitats Directive and the "Natura 2000"), and a timely and constant production of updated coverages maps is required. Traditional techniques for vegetation map production are based on time consuming and expensive field surveys and direct observations [1] or manual comparison of images. The average vegetation canopies (e.g., deciduous shrubs, deciduous trees, grasslands) are complex mixes of interviewed species life cycles marked by different stages of growth and senescence, each one with different leaves colors and photosynthetic activity [2]. Recurring changes in foliage affects the electromagnetic radiation reflectance of surfaces captured by the sensors [3]. The timing recurring reflectance changes of bio-surfaces under a changing environment is known as land surface phenology (LSP) [4].

In this context, our experiment aims at testing a fast time and less expensive method to get to a classification of forest categories using a set of three-year-set Sentinel-2 Images in Google Earth Engine (GEE; https://earthengine.google.com) [5] from 2018 to 2020, in a case study in center Italy. The Earth Engine service can be joined by APIs (Application Programming Interfaces). Client libraries for JavaScript and Python translates complex geospatial analyses into Earth Engine requests, the REST API connects to the Earth Engine servers [6]. Time-series generated for each category allow for identifying the specific class composition verified by ground truths. Principal Component Analysis (PCA) was used to reduce output data redundancy, pruning the variable set composition, before the Random Forest [7] supervised classification.

As shown in Fig. 1, the case study, Forest of Arcevia, is located in central Italy in the Apennines (43°30′36.71″N 12°55′02.98″E, WGS84). With an area of 990 ha at 752 m above sea level, the study area is characterized by four dominant forest categories: Holm oak woods, Conifer reforestation, Mixed hardwood woods, and Orno ostryenion woods.

The area was reforested using *Pinus nigra* J.F. Arnold, an alien species that has been planted for protective purposes in the post-war period. Being an allochthonous species, its natural regeneration suffers from competition. Due to the lack of management or of specific intervention polices, the autochthonous vegetation recolonized most of the area. The abandonment also favored the development of local floras under the forest understory, which currently is composed by a mixture of deciduous broad-leaved species usually present in the area. A monitoring key issue is linked to the spectral signature responses to that peculiar structure characterized by an upper *P. nigra* canopy and the lower deciduous forest understory.

Considering these categories, the classification [8] had been carried out, as described in the following paragraphs.

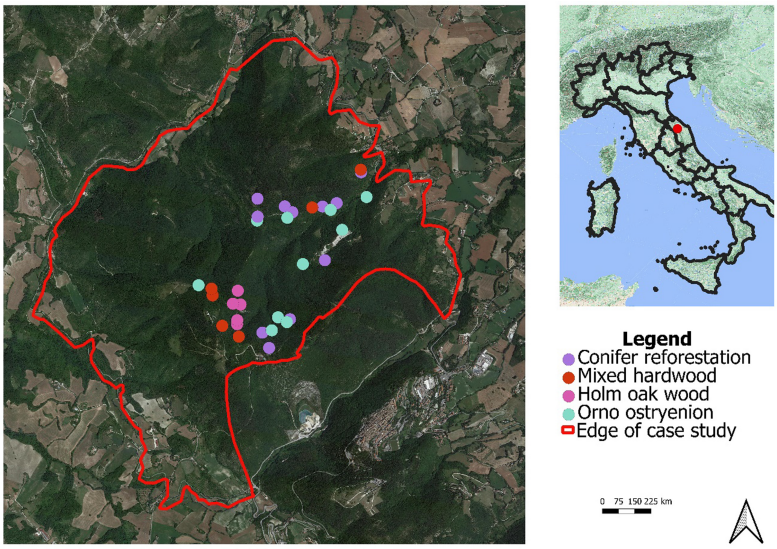

Fig. 1. The location of the study area and the points surveyed on the ground using a GNSS, to collect the Region of Interests as ground truths.

2 Materials and Methods

The Sentinel-2 Images set considered for in this study, is a product of the European Space Agency (ESA) Copernicus Service. The Sentinel-2A and Sentinel-2B platforms are operational since 2015 and 2017 respectively [9]; whose scopes ranges from land management [10], agriculture and forestry [11], up to disaster control, humanitarian relief operations, risk mapping [12] and security. The Sentinel-2 mission is equipped with Multi-Spectral Instrument (MSI), sampling 13 spectral bands, each with its own

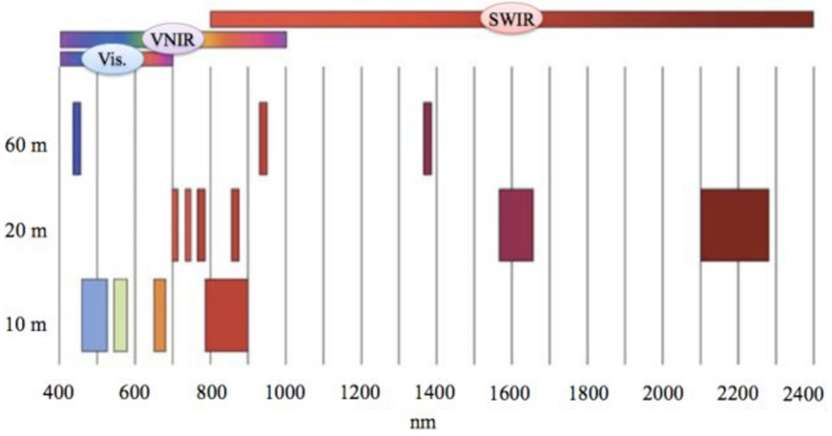

Fig. 2. Sentinel-2 10, 20 and 60 m spatial resolution bands: B1 (443 nm), B2 (490 nm), B3 (560 nm), B4 (665 nm), B5 (705 nm), B6 (740 nm), B7 (783 nm), B8 (842 nm), B9 (940 nm), B10 (1375 nm), B11 (1610 nm) and B12 (2190 nm) [13] (Color figure online)

specific spatial resolution. According to the literature, we opted for a bands composition commonly used in forest mapping, the bands n. 2,3,4 and 8 with a spatial resolution of 10 m on the ground. Blue, Green, Red and Near InfraRed (NIR), respectively, as showed in Fig. 2. Usually, the Copernicus Service offers atmospheric corrected open access data, in our case we could acquire the Level-1C and Level-2A, corrected by Top-Of-Atmosphere (TOA).

The chosen satellite bands have been processed by GEE [14], a geospatial data storage, analysis and visualization service powered by the Google Cloud Platform [15]. In spite of its lower spatial resolution, Sentinel-2 allows reliable forest classifications if the forest has a simple structure, composed by few different species [16].

Figure 3 shows the flowchart up to the final classification map outputs, provided with the specific accuracy metrics.

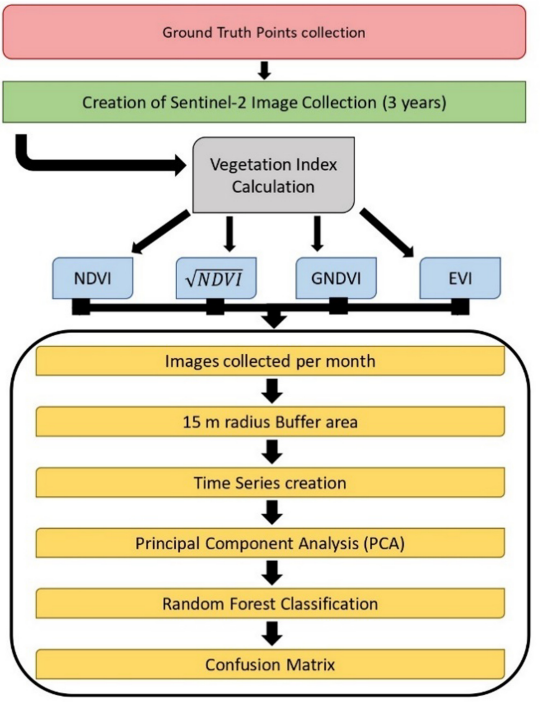

Fig. 3. Workflow of purposed method for forest mapping.

Firstly, the study area and the ground truth points have been uploaded in the Code Editor as vector data. The Copernicus Sentinel-2A dataset was also got into the Code Editor filtering by location, date, and cloud coverage, considering a threshold of less than 50% for this latter. A single monthly image was chosen each year at the end of the iterative process. The Vegetation Indexes (VIs) have been calculated and turned into bands in the GEE platform [17] as follow: Normalized Difference Vegetation Index (NDVI) [18, 19], Transformed Difference Vegetation Index (TDVI) [20], Enhanced Vegetation Index

(EVI) [21] and the Green Normalized Difference Vegetation Index (GNDVI) [22]. The following are the formulas used to calculate the different VIs:

$$\text{NDVI} = \frac{NIR - RED}{NIR + RED}$$

$$TDVI = \sqrt{\frac{NIR - RED}{NIR + RED} + 0.5}$$

$$\text{EVI} = \frac{NIR - RED}{NIR + C1 \cdot RED - C2 \cdot BLUE + L'}$$

$$\text{GNDVI} = \frac{NIR - GREEN}{NIR + GREEN}$$

Considering the images analyzed in these time series, the overcome are showed in Fig. 4, 5 and 6.

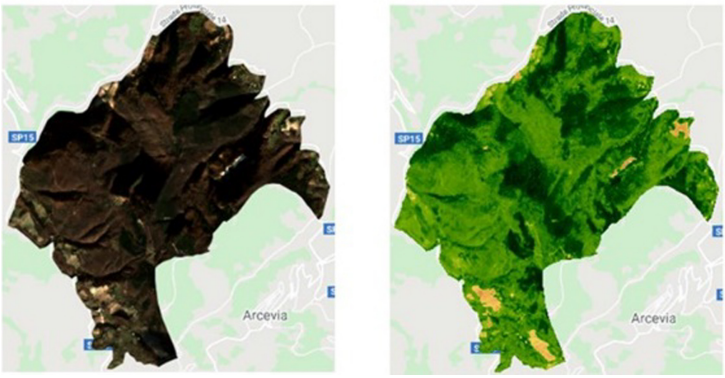

1 2

Fig. 4. The output stock images by vegetation indices computed in: 1) January 2018 RGB image; 2) January 2018 mean NDVI..

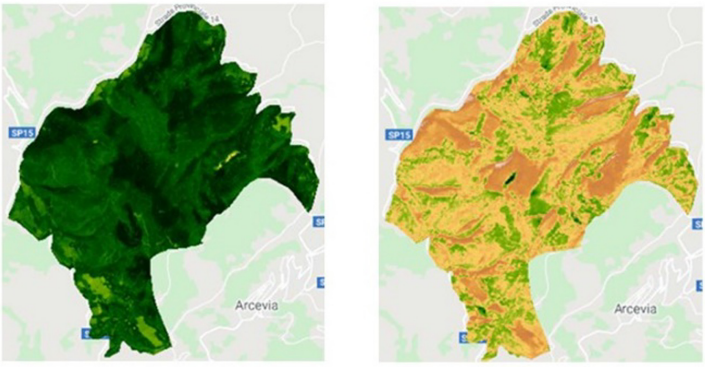

3 4

Fig. 5. The output stock images by vegetation indices computed in: 3) January 2018 mean Transformed Difference Vegetation Index (TDVI) and 4) January 2018 mean EVI



Fig. 6. The output stock images computed in January 2018: mean GNDVI.

The output images collection has been gathered per month, and the average monthly VIs values have been recorded each year. The surveyed ground truth points (see Fig. 1) have been buffered considering a radius of 15 m to verify the presence of the same category within the buffer area. Each pixel falling within the buffer has been converted into a "feature", recording the pixel's coordinates (Latitude and Longitude) as features properties. By plot each pixel time pattern as a single random color line during the twelve months, we have produced the time-series charts of each VI (Figs. 7, 8, 9 and 10). The charts allow for identifying the different phenological behaviors [23] along with the various forest categories. The holm oak wood showed an almost constant NDVI value throughout the year, whereas the others three categories have reached a minimum in the first months of the year and a maximum during the spring and the summer.

The computational time for modelling was shortened, reducing the number of variables performing by Principal Component Analysis (PCA) [24]. Essentially, PCA represents a transformation of original variables into a new orthogonal reference system, with fewer variables, where the variable with higher variance is projected on the first axis, the second invariance on the second, and so on.

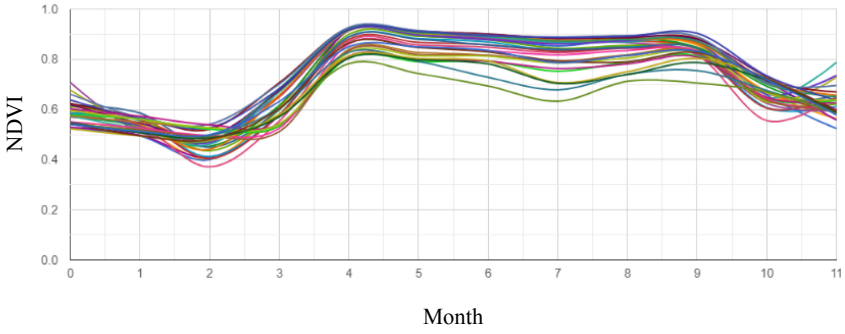

Fig. 7. The Mixed hardwood NDVI monthly time series.

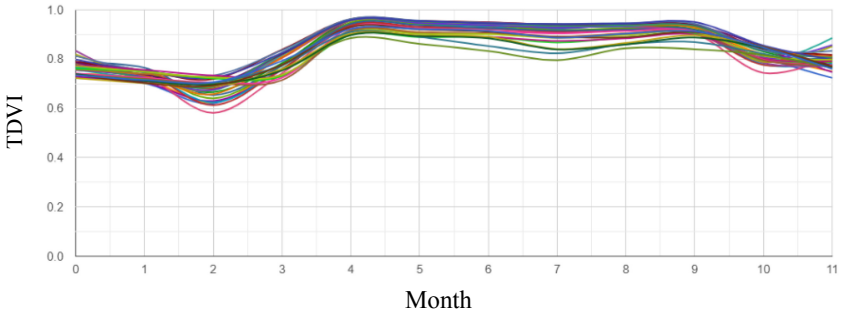

Fig. 8. The Mixed hardwood TDVI monthly time series.

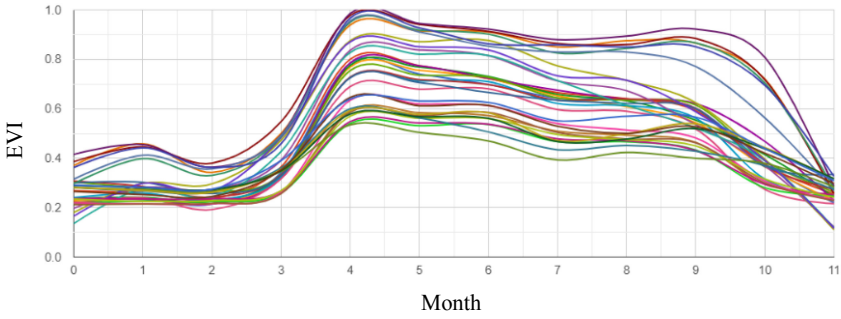

Fig. 9. The Mixed hardwood EVI monthly time series

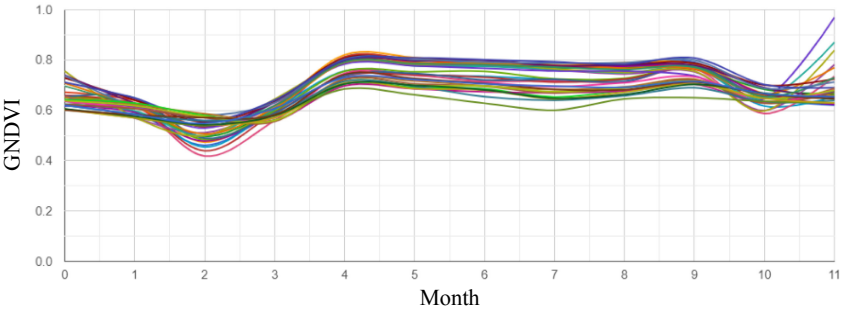

Fig. 10. The Mixed hardwood GNDVI monthly time series

PCA results are called scores and represent the "coordinates" of each point in the new reference system. PC1 and PC2 (the first two principal components) can be used to define the reduced phenological ordination space of ground truth known locations. The plot of PC1 and PC2, called score plot, support the interpretation of a distinct forest plant community phenology [25], showing clusters of samples (plant associations) based on their similarity. Close samples have a similar composition, whereas distant samples

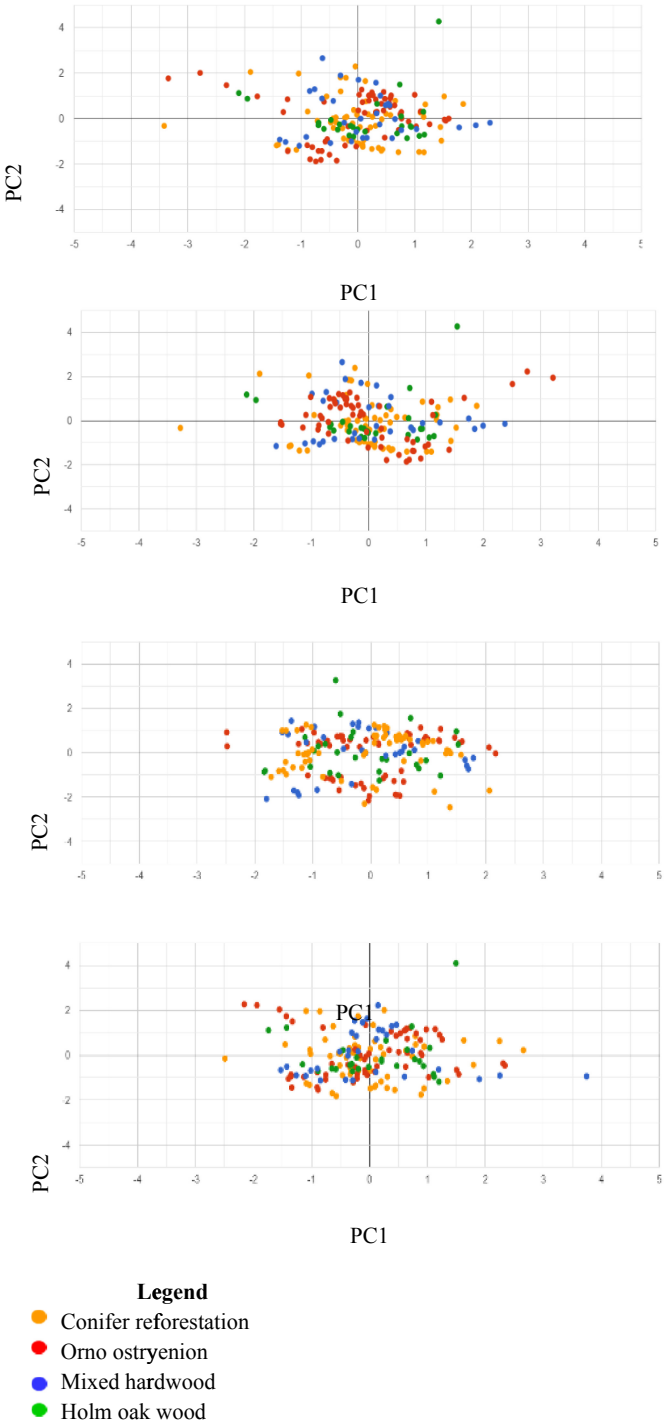

Fig. 11. The PCA scores show a cluster of plant associations based on following Vis

are much different from each other. To provide a score plot for each plant association, the first two principal component values of pixels belonging to a buffered region have been extracted. As shown in Fig. 11, the EVI shows values gathering along both axes compared with other indexes. On the other hand, these latter ones show a relatively uniform pattern among the different forest categories.

The classification was performed by Random Forest (RF) [7], a supervised learning method. To perform the RF, the number of classification trees has been set to 500 and the number of input variables used at each split node has been set to 2, which are the default setting of this classifier. In this case, the presence of ground truth points "supervises" the process of pixel classification by training the model with data on plant associations, verified in the field by direct observation. Then, the computer algorithm uses values from training areas (or points) to classify the whole image, predicting the same forest category in each pixel. It is necessary to divide the dataset into two parts for the classification model creation: "training-set" to perform the system training and "test-set" to try the algorithm accuracy. The GEE scripts allowed for splitting the dataset along with a specific percentage, with "training points" as 30% of the total and the "validation points" the remaining 70%. Indeed, to assure a "fair" assessment of a classifier's generalization, the training data must be separated from data to assess accuracy [26]. Each forest category has its own class number, in which Class 0 are the Holm oak woods, Class 1 the Conifer, Class 3 the Mixed Hardwood forest and Class 3 the Orno-ostryenion association.

3 Experiment Results and Discussion

This paragraph describes the output confusion matrices based on training data. Moreover, the results of the overall training accuracy are computed. The algorithm accuracy was validated by a test-set, assessing the classification's error through independent data. The error matrix and accuracy are matrices comparing two columns of the validated test-set: one containing the actual values and the other the predicted values. The matrix rows correspond to the actual values, whereas the columns to the predicted values. The obtained accuracies are calculated utilizing the confusion matrices obtained for each VI, as shown in the Table 1 [27].

The maximum classification accuracy is reached using NDVI and GNDVI, the most frequent VIs in literature, thanks to their ability to enhance the reflectance between the Red/Green and the NIR bands. The principle behind the chosen VIs for forest classifications is that the vegetation shows a higher reflectance in the NIR, than other bands. This contrast has been used as a proxy of the vegetation healthy status VIs are indeed biophysical parameters, related to the photosynthetic activities. The analysis of the time-series composed by different images in different periods offers valuable information to monitoring the forest dynamics [28].

The experiment has proven to be effective, as shown by the accuracy threshold of the confusion matrix. NDVI and GNDVI are within the range of 84%, while the TDVI is 81%, and EVI is 78%, as it is possible to observe in Table 1. These results show that Sentinel-2 free images can be safely used to classify different forest categories over a large area, even with limited input sample data collected on the ground.

Table 1. The consumer accuracy values using different Vegetation Indices as Input into Random Forestry. The different tree species are noted as follow: 0 = Holm oak wood, 1 = Conifer reforestation, 2 = Mixed hardwood, 3 = Orno ostryenion

NDVI					
Class	0	1	2	3	User accuracy
0	7	0	0	0	1
1	3	20	0	0	0.87
2	0	0	9	4	0.69
3	0	0	3	17	0.85
Producer Accuracy	0.70	1	0.75	0.81	
Validation overall accuracy: 0.84					

TDVI					
Class	0	1	2	3	User Accuracy
0	7	0	0	0	1
1	3	20	2	0	0.80
2	0	0	7	4	0.64
3	0	0	3	17	0.85
Producer Accuracy	0.70	1	0.58	0.81	
Validation overall accuracy: 0.81					

EVI					
Class	0	1	2	3	User accuracy
0	9	0	0	0	1
1	1	20	5	3	0.69
2	0	0	4	2	0.67
3	0	0	3	16	0.84
Producer Accuracy	0.90	1	0.33	0.76	
Validation overall accuracy: 0.78					

GNDVI					
Class	0	1	2	3	User Accuracy
0	8	0	0	0	1
1	2	20	2	0	0.83
2	0	0	7	3	0.70
3	0	0	3	18	0.86
Producer Accuracy	0.80	1	0.58	0.86	
Validation overall accuracy: 0.84					

The use of PCA allows for a higher classification accuracy of forest areas. According to Xu et al. [29] an overall accuracy of more than 82% was obtained using NDVI to a forest species classification of five classes. Gimire et al. [30] employed RF to mapping the variety of tree species, using time-series of wooded landscapes, obtaining an overall accuracy of 78% for EVI. Praticò et al. [15] created a stack of images of all the Sentinel-2 bands and added the computation of the GNDVI index, obtaining an overall accuracy of 86%.

Noteworthy, there is no literature about similar workflow employing the TDVI index. Therefore, in accordance with these authors, the obtained results are in line with those achieved by their research team.

Moreover, looking at the classification results for each different vegetation index shown in Fig. 12, it is possible to observe that all the classified maps have a similar pattern but the case n. 3, shows a limited holm oak wood area and a large conifers' reforestation area if compared with the other outputs. This result, in our study, indicates a lesser effectiveness of EVI to clearly represent the phenological behaviour of the 4 forest categories.

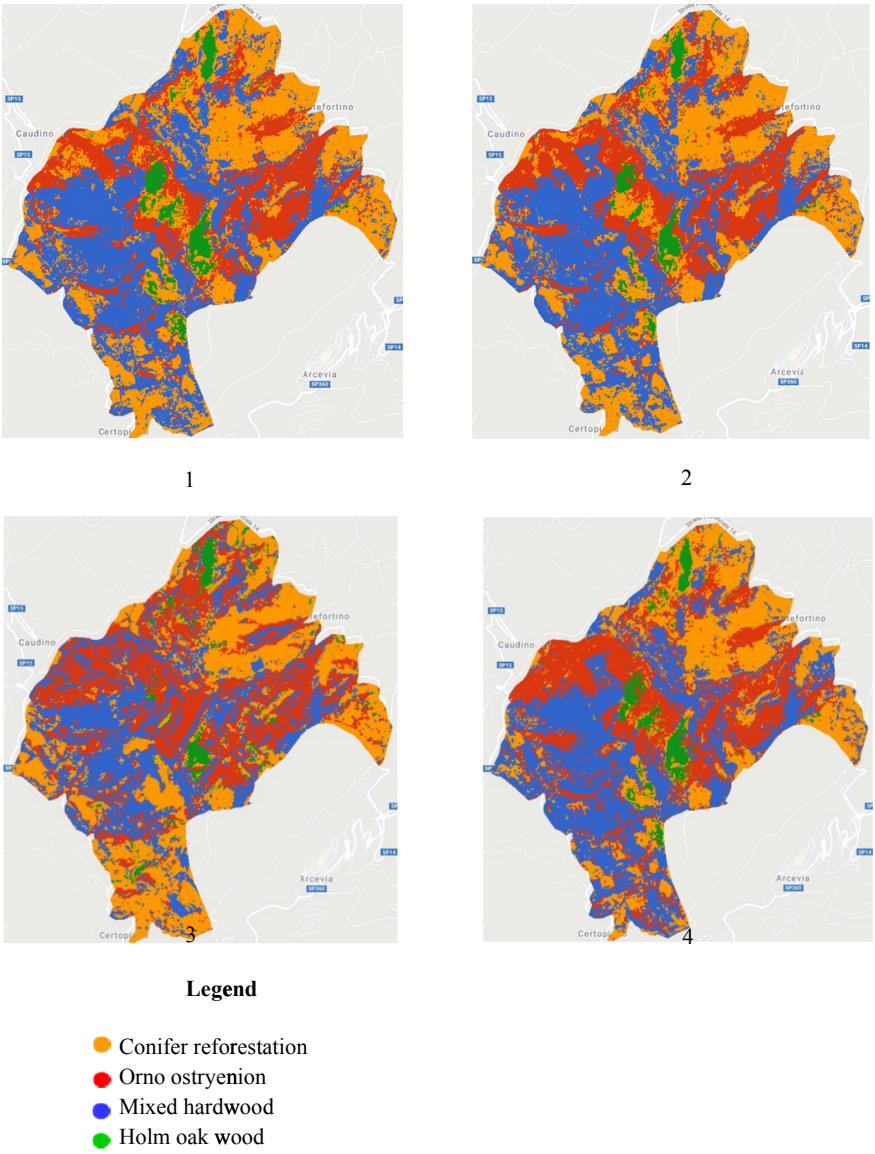

Fig. 12. Image classification by Random Forest algorithm: 1) NDVI; 2) TDVI; 3) EVI; 4) GNDVI.

4 Conclusion

The increasing availability of earth observation data and satellite missions with a wide range of spectral sets at different spatial resolutions offers the opportunity to map large forest areas in less time-consuming ways. Researchers are constantly looking at improved and ground-breaking workflows and methods. The aim is to obtain accurate and reliable representations and classification of the forest categories analyzed in a certain area. This study examined different vegetation indexes through a time-series composed by Sentinel-2 images stack over 4 years on GEE platform. The methodology described in this paper reduce the seasonal variability of the vegetation data, lowering the effect of external variables (such as the presence of plant pathologies or different climate phenomena). These steps showed that not all VIs are able to achieve a high global accuracy. Indeed, the automatic mapping of complex wooden areas, is a complex activity.

Our commitment for future researches is to repeat this kind of approach, with the opportunity to test other free satellite platforms, such as Landsat-8 (NASA - USGS) or commercial constellations such as PlanetScope [31] Thanks to the integration of these platforms with machine learning (ML) and deep learning (DL) methodologies for forest mapping, there will be the possibility to evaluate scores from traditional or innovative algorithms. Among the ML ones, K-Nearest Neighbors (KNN) [32], Support Vector Machine (SVM) [33], Classification and Regression Tree (CART) [34] and eXtreme Gradient Boosting (XGBoost) are the most represented in literature [35], while among the DL ones it is possible to use the Fusion of Spectral image and Point data (FSP) method [36] which is based on the Kullback–Leibler divergence (KL), on the curve angle mapper (CAM) or on the root sum squared differential area (RSSDA) curve matching classifiers. These algorithms are able to improve the accuracies of automatic classification for different forest categories, making easier this analysis in different mixed tree species context.

References

1. Choudhury, A.M., et al.: Urban tree species identification. Forest **11**, 22 (2020). https://doi.org/10.3390/f11111226
2. Di Fazio, S., Modica, G., Zoccali, P.: Evolution trends of land use/land cover in a mediterranean forest landscape in Italy. In: Murgante, B., Gervasi, O., Iglesias, A., Taniar, D., Apduhan, B.O. (eds.) Computational Science and Its Applications - ICCSA 2011, pp. 284–299. Springer, Heidelberg (2011). https://doi.org/10.1007/978-3-642-21928-3_20
3. Vogelmann, J.E., Xian, G., Homer, C., Tolk, B.: Monitoring gradual ecosystem change using landsat time series analyses: case studies in selected forest and rangeland ecosystems. Remote Sens. Environ. **122**, 92–105 (2012). https://doi.org/10.1016/j.rse.2011.06.027
4. Mondal, P., Liu, X., Fatoyinbo, T.E., Lagomasino, D.: Evaluating combinations of sentinel-2 data and machine-learning algorithms for mangrove mapping in West Africa. Remote Sens. **11**(24), 2019. https://doi.org/10.3390/rs11242928
5. Gorelick, N., Hancher, M., Dixon, M., Ilyushchenko, S., Thau, D., Moore, R.: Google earth engine: planetary-scale geospatial analysis for everyone. Remote Sens. Environ. **202**(2016), 18–27 (2017). https://doi.org/10.1016/j.rse.2017.06.031
6. Kumar, L., Mutanga, O.: Google earth engine applications since inception: usage, trends, and potential. Remote Sens. **10**(10), 1–15 (2018). https://doi.org/10.3390/rs10101509

7. Breiman, L.: Random forests. Mach. Learn. 1–28 (2001). https://doi.org/10.1201/9780429469275-8.
8. Modica, G., Merlino, A., Solano, F., Mercurio, R.: An index for the assessment of degraded mediterranean forest ecosystems. For. Syst. **24**(3) (2015). https://doi.org/10.5424/fs/2015243-07855.
9. Copernicus, E.: The European Space Agency - Sentinel. https://sentinel.esa.int/web/sentinel/missions/sentinel-2.
10. Gulinck, H., et al.: The fourth regime of open space. Sustain. **10**(7), 1–15 (2018). https://doi.org/10.3390/su10072143
11. Li, J., Wang, L.: Forest type classification with multitemporal sentinel-2 data. In: Proceedings - IEEE Congress on Cybermatics, IEEE International Conferences on Internet of Things, iThings 2020, IEEE green computing and communications, greencom 2020, IEEE cyber, physical and social computing, CPSCom 2020 and IEEE smart data. SmartD 2020, pp. 498–504 (2020). https://doi.org/10.1109/iThings-GreenCom-CPSCom-SmartData-Cybermatics50389.2020.00091
12. Solano, F., Colonna, N., Marani, M., Pollino, M.: Geospatial analysis to assess natural park biomass resources for energy uses in the context of the Rome metropolitan area. In: Calabrò, F., Della Spina, L., Bevilacqua, C. (eds.) ISHT 2018. SIST, vol. 100, pp. 173–181. Springer, Cham (2019). https://doi.org/10.1007/978-3-319-92099-3_21
13. Regan, A., Silvestrin, P., Fernandez, D., Gabriele, A., Leveque, N.: Sentinel convoy: synergetic observations with satellites flying in formation with European Operational Missions. In: Proc. 4S Symp. Small Satell. Syst. Serv. January, pp. 1–12 (2010)
14. Chung, L.C.H., Xie, J., Ren, C.: Improved machine-learning mapping of local climate zones in metropolitan areas using composite Earth observation data in Google Earth Engine. Build. Environ. **199**(15), 107879 (2021). https://doi.org/10.1016/j.buildenv.2021.107879
15. Praticò, S., Solano, F., Di Fazio, S., Modica, G.: Machine learning classification of mediterranean forest habitats in google earth engine based on seasonal sentinel-2 time-series and input image composition optimisation. Remote Sens. **13**(4), 1–28 (2021). https://doi.org/10.3390/rs13040586
16. Wessel, M., Brandmeier, M., Tiede, D.: Evaluation of different machine learning algorithms for scalable classification of tree types and tree species based on Sentinel-2 data. Remote Sens. **10**(9), 1419 (2018). https://doi.org/10.3390/rs10091419
17. Tassi, A., Vizzari, M.: Object-oriented lulc classification in google earth engine combining snic, glcm, and machine learning algorithms. Remote Sens. **12**(22), 1–17 (2020). https://doi.org/10.3390/rs12223776
18. Hanes, J.M. (ed.): Biophysical Applications of Satellite Remote Sensing. SRS, Springer, Heidelberg (2014). https://doi.org/10.1007/978-3-642-25047-7
19. Choudhury, M.A.M., Marcheggiani, E., Galli, A., Modica, G., Somers, B.: Mapping the urban atmospheric carbon stock by lidar and worldview-3 data. Forests **12**(6), 692 (2021). https://doi.org/10.3390/f12060692
20. Tsafack, N., Fattorini, S., Frias, C.B., Xie, Y., Wang, X., Rebaudo, F.: Competing vegetation structure indices for estimating spatial constrains in carabid abundance patterns in chinese grasslands reveal complex scale and habitat patterns. Insects. **11**(4), 249 (2020). https://doi.org/10.3390/insects11040249
21. Choubin, B., et al.: Effects of drought on vegetative cover changes: investigating spatiotemporal patterns, Elsevier Inc. **2**, 213–222 (2019)
22. Isip, M.F., Alberto, R.T., Biagtan, A.R.: Exploring vegetation indices adequate in detecting twister disease of onion using Sentinel-2 imagery. Spat. Inf. Res. **28**(3), 369–375 (2019). https://doi.org/10.1007/s41324-019-00297-7

23. Pesaresi, S., Mancini, A., Quattrini, G., Casavecchia, S.: Mapping mediterranean forest plant associations and habitats with functional principal component analysis using Landsat 8 NDVI time series. Remote Sens. **12**(7), 1132 (2020). https://doi.org/10.3390/rs12071132
24. Macintyre, P., van Niekerk, A., Mucina, L.: Efficacy of multi-season Sentinel-2 imagery for compositional vegetation classification. Int. J. Appl. Earth Obs. Geoinf. **85**, 101980 (2020). https://doi.org/10.1016/j.jag.2019.101980
25. Pesaresi, S., Mancini, A., Casavecchia, S.: Recognition and characterization of forest plant communities through remote-sensing NDVI Time Series divers. **2**(8), 1–192 (2011). https://doi.org/10.3390/d12080313.
26. Goldblatt, R., You, W., Hanson, G., Khandelwal, A.K.: Detecting the boundaries of urban areas in India: a dataset for pixel-based image classification in google earth engine. Remote Sens. **8**(8), 634 (2016). https://doi.org/10.3390/rs8080634
27. Stehman, S.V., Foody, G.M.: Key issues in rigorous accuracy assessment of land cover products. Remote Sens. Environ. **231**, 111199 (2019). https://doi.org/10.1016/j.rse.2019.05.018
28. Xie, Y., Sha, Z., Yu, M.: Remote sensing imagery in vegetation mapping: a review. J. Plant Ecol. **1**(1), 9–23 (2008). https://doi.org/10.1093/jpe/rtm005
29. Xu, K., Tian, Q., Zhang, Z., Yue, J., Te Chang, C.: Tree species (Genera) identification with GF-1 time-series in a forested landscape, Northeast China. Remote Sens. **12**(10), 1–18 (2020). https://doi.org/10.3390/rs12101554
30. Ghimire, B.R., Nagai, M., Tripathi, N.K., Witayangkurn, A., Mishara, B., Sasaki, N.: Mapping of Shorea robusta forest using time series MODIS data. Forest **8**(10), 384 (2017). https://doi.org/10.3390/f8100384
31. Parente, L., Taquary, E., Silva, A.P., Souza, C., Ferreira, L.: Next generation mapping: combining deep learning, cloud computing, and big remote sensing data. Remote Sens. **11**(23), 2881 (2019). https://doi.org/10.3390/rs11232881
32. Zhang, Z.: Introduction to machine learning: K-nearest neighbors. Ann. Transl. Med. **4**(11), 1–7 (2016). https://doi.org/10.21037/atm.2016.03.37
33. Cortes, C., Vapnik, V.N.: Support-vector networks. Mach. Learn. **20**, 273–297 (1995). https://doi.org/10.1023/A:1022627411411
34. Breiman, L., Friedman, J.H., Olshen, R.A., Stone, C.J.: Classification and Regression Trees. Chapman & Hall/CRC (1984)
35. Karasiak, N., Sheeren, D., Fauvel, M., Willm, J., Dejoux, J.F., Monteil, C.: Mapping tree species of forests in southwest France using Sentinel-2 image time series. In: 2017 9th Int. Work. Anal. Multitemporal Remote Sens. Images, MultiTemp 2017, pp. 1–4. Brugge, Belgium (2017). https://doi.org/10.1109/Multi-Temp.2017.8035215.
36. Wan, H., Tang, Y., Jing, L., Li, H., Qiu, F., Wu, W.: Tree species classification of forest stands using multisource remote sensing data. Remote Sens. **13**(1), 1–24 (2021). https://doi.org/10.3390/rs13010144